JOURNAL OF CATALYSIS 133, 415–430 (1992)

Surface Structure of Crystalline and Amorphous Chromia Catalysts for the Selective Catalytic Reduction of Nitric Oxide

II. Diffuse Reflectance FTIR Study of Thermal Treatment and Oxygen Adsorption

M. SCHRAML-MARTH,* A. WOKAUN,[1,*] H. E. CURRY-HYDE,[2,†] AND A. BAIKER†

*Physical Chemistry II, University of Bayreuth, D-W-8580 Bayreuth, Germany; and †Department of Chemical Engineering and Chemical Technology, Swiss Federal Institute of Technology, ETH Zentrum, CH-8092 Zürich, Switzerland

Received February 27, 1991; revised July 29, 1991

The activation of crystalline and amorphous chromia surfaces by thermal pretreatment in argon and oxygen adsorption at 473 K has been studied by diffuse reflectance FTIR and Raman spectroscopy. The formation of coordinatively unsaturated chromium sites during thermal activation is monitored by observing the evolution of Cr=O stretching absorptions both in the fundamental and overtone regions of the FTIR spectrum. On α-Cr_2O_3, labile surface oxygen species are largely removed at 498 K, whereas on the amorphous chromia surface, labile oxygen is more tightly bound. As a consequence, coordinatively unsaturated chromium sites are generated on amorphous chromia to a lesser extent than on α-Cr_2O_3. Upon high-temperature oxygen treatment, O_2 is dissociatively adsorbed. Coordinatively unsaturated sites are occupied by the added oxygen, as manifested by an increase in the number of Cr=O oscillators. Fine structure in the Cr=O absorptions of the amorphous chromia is observed for the first time, and is tentatively assigned to various types of surface sites. Raman spectroscopic characterization of the amorphous chromia surface reveals laser-induced dehydration and creation of coordinatively unsaturated surface Cr=O sites, accompanied by progressive crystallization of the amorphous substrate. Differences between crystalline and amorphous chromia with respect to their SCR activity are correlated with the higher density of labile oxygen species available on the surface of amorphous chromia under SCR reaction conditions (423–473 K).

1. INTRODUCTION

In search for new catalysts for the selective catalytic reduction (SCR) of nitric oxide with ammonia, crystalline and supported chromia have been studied by several authors (*1*). The morphology of the catalyst has a significant influence on the performance in the SCR reactions

$$4NO + 4NH_3 + O_2 \rightarrow 4N_2 + 6H_2O$$

and

$$6NO + 4NH_3 \rightarrow 5N_2 + 6H_2O,$$

as shown by a recent comparison (*2*) of crystalline and amorphous chromia with respect to their SCR activity and selectivity. Under the conditions specified in Ref. (*2*), complete conversion of NO was achieved at 155°C over amorphous chromia, whereas over crystalline chromia the conversion was only 15% at the same temperature. The specific rate of nitric oxide conversion referred to the BET area of the amorphous sample was four times higher than that of crystalline chromia (*2*). Noteworthy differences exist in the selectivity patterns of the two samples. Amorphous chromia produces N_2 almost exclusively at 155°C even at full conversion; in contrast, on crystalline chromia the N_2 selectivity only amounts to one-third, with the rest of the nitrogen being released as N_2O.

[1] To whom correspondence should be addressed.

[2] Present address: School of Chemical Engineering and Industrial Chemistry, University of New South Wales, PO Box 1, Kensington, 2033, Australia.

0021-9517/92 $3.00

This difference in performance must be related to the existence of morphological differences between crystalline and amorphous chromia, as evidenced by the TPD experiments reported in part I of this study (*3*). To further elucidate these differences and to promote our understanding of the catalytic reaction mechanism, we have used diffuse reflectance FTIR (DRIFT) and Raman spectroscopy to study the thermal activation of chromia surfaces, the binding of oxygen and ammonia, as well as the adsorption of nitric oxides. In part II of this study, the influence of thermal pretreatment on the active sites present on the chromia surface is investigated, with special attention paid to labile oxygen species that are formed in the course of this process. Subsequently, oxygen is chemisorbed on the activated surface, and changes in the chromium-bound oxygen species present on the surface are monitored. Ammonia adsorption experiments on catalysts activated by this pretreatment will be described in part III.

1.1. Crystalline Chromia

Bulk crystalline chromia (α-Cr_2O_3), as well as various types of supported chromia, have been studied using a variety of techniques (*4*). Special interest has been devoted to the detection and characterization of active sites that develop during catalyst pretreatment. Burwell *et al.* (*4*) have proposed that these sites consist of coordinatively unsaturated Cr^{3+} ions formed by loss of water. It is generally accepted (*5*) that the coordinatively unsaturated centers, together with Brønsted acidic sites, are important in a variety of catalytic reactions on chromia surfaces (cf. (*4*), and references therein).

Shchekochikhin *et al.* (*6*), as well as Davydov *et al.*(*7*), have used IR spectroscopy to study O_2 adsorption onto α-Cr_2O_3 prepared by thermal decomposition of $(NH_4)_2Cr_2O_7$. After thermal activation in air at 873 K for 2 h, no bands were detected in the range between 700 and 1200 cm^{-1}, where characteristic absorptions due to Cr–O vibrations, with bond orders between 1 and 2, are expected (*8*). Adsorption of O_2 at room temperature led to a broad and weak feature at 985 cm^{-1}. Upon oxygen adsorption at higher temperatures (523 K) intensive bands at 1015, 995, and 980 cm^{-1} were formed, together with weaker broad features at 890 and 820 cm^{-1}. Subsequent thermal treatment at 643 K caused the disappearance of all bands except the one at 1015 cm^{-1}; at 873 K no absorptions remained. The adsorption of ethanol and water at room temperature resulted in the disappearance of the high-frequency bands at 1015 and 995 cm^{-1}, while at 473 K and higher EtOH or H_2O partial pressures all bands vanished.

Metal–oxygen double bonds, M=O, absorb between 900 and 1200 cm^{-1} (*8*). The authors of studies (*6, 7*) therefore conclude that oxygen is dissociatively chemisorbed, and assign the bands at 1015, 995, and 980 cm^{-1} to different types of Cr=O groups with bond orders close to 2. The band at 890 cm^{-1} is close in frequency to one of the absorptions of Cr(VI)oxide (970 and 893 cm^{-1}), and is therefore assigned to a surface structure analogous to CrO_3. The bands that exhibit the highest thermal stability (1015 and 995 cm^{-1}) are most sensitive to EtOH and H_2O adsorption, which was attributed to a higher degree of coordinative unsaturation with respect to oxygen, as compared to the less affected bands at 985, 890, and 820 cm^{-1}.

Zecchina *et al.*(*9*) have studied O_2 adsorption on a surface of α-Cr_2O_3 that was completely dehydroxylated by reduction at 673 K in an excess of CO. Oxygen adsorption at room temperature produced three groups of IR absorptions at 1040–970, 900–880, and 850–750 cm^{-1}. The first group was most intensive at room temperature, and consisted of five components. The relative intensity of the highest frequency peaks was found to depend on the dehydration of the surface. This dependence was tested by rehydroxylation, activation, and oxygen adsorption at different temperatures. As no O_2 was evolved, Zecchina *et al.* (*9*) concluded that a surface rearrangement was taking place,

during which selected species were transformed into others of a higher stability. Individual Cr=O stretching frequencies were interpreted in terms of a scheme presented below in Section 2. Bands in the range between 900 and 880 cm^{-1} were attributed to normal modes of *M*—O—*M* groups present in $(CrO_4)^{x-}$-type polymeric structures, formed by surface rearrangements at higher temperatures.

Carrot and Sheppard (*10*) have reinvestigated the activation of crystalline chromia described in Ref. (*9*). Upon oxygen adsorption at room temperature they observed bands at 1023, 1015, 995(s), 986, and 980 cm^{-1}, in close agreement with Zecchina *et al.* (*9*). Studies involving ^{16}O and ^{18}O isotopes led to the conclusion that the bands in the 1030 to 940 cm^{-1} range can be assigned to mono-oxygen Cr=O surface species.

1.2. Amorphous Chromia

Upon slow precipitation from Cr^{3+} solutions a green gel $(Cr(OH)_3(H_2O)_3)_x$ is formed (*11*). Drying of the gel and calcination in inert atmosphere between 473 and 673 K results in the removal of water and the formation of a black X-ray amorphous material, according to

$$2Cr(OH)_3(H_2O)_3 \rightarrow Cr_2O_3 \cdot xH_2O + (9 - x)H_2O.$$

The amorphous chromia is structurally similar to chromium–trihydroxide–trihydrate, with some H_2O ligands replaced by bridging O^{2-} or OH^- ligands. In the trihydrate the coordination number of the Cr^{3+} is 6, whereas the coordination number of oxygen is unity. In crystalline chromia, on the other hand, the coordination number of Cr^{3+} is 6 as well, but the coordination number of oxygen rises to 4. Upon drying a hydrous chromium hydroxide gel, the oxygen coordination number successively rises from 1 to 4 with increasing calcination temperature (*4*).

Singh *et al.* (*12*) have studied the structural evolution during calcination of amorphous chromia. From EXAFS experiments the authors conclude that the first coordination sphere of Cr^{3+} consists of six oxygen ligands. Upon heating Cr—OH groups condense to form Cr—O—Cr bridges, without change of the chromium coordination number. This dehydration process results in microcrystalline α-Cr_2O_3 particles.

Temperature-programmed reaction and desorption (TPRD) experiments have been reported in part I of this study (*3*). Thermoanalytic measurements on amorphous Cr_2O_3 have been performed by Singh *et al.* (*12*) and Ratnasamy and Leonard (*13*). An endothermic DSC peak at 423 K accompanied by a weight loss of 3–4% was attributed to the desorption of loosely bound water molecules. An additional weak endothermic feature around 523 K was attributed to a loss of water by condensation of surface hydroxyl groups (cf. Section 2). Finally, crystallization at 683 K yielding α-Cr_2O_3 is accompanied by a weight loss of 5–6% due to desorption of crystal water.

Infrared spectroscopic studies have been performed by Zecchina *et al.* (*9*), Singh *et al.* (*12*), and Ratnasamy and Leonard (*13*). Broad absorptions in the 1000–700 cm^{-1} range have been partly attributed (*9*) to the bending modes of surface hydroxyl groups.

2. MODEL FOR THE CHROMIA SURFACE

To interpret the spectroscopic results presented below, a model for the chromia surface based on the proposal of Burwell *et al.* (*4*) will be used. According to Scarno *et al.* (*14*), as well as other authors (*9, 15*), the (001) face is the most abundant on α-Cr_2O_3. We therefore confine the discussion to this surface; other crystallographic faces have been considered by Burwell *et al.* (*4*).

The crystal structure of α-Cr_2O_3 corresponds to a hexagonal close-packed lattice of oxide ions, with two-thirds of the octahedral holes occupied by Cr^{3+} ions. Consider an (001) cleavage parallel to a closely packed plane of the crystal, and distribute oxygen ions in the surface layer in such number that charge neutrality is preserved. Then every Cr^{3+} ion in the layer underneath these oxide

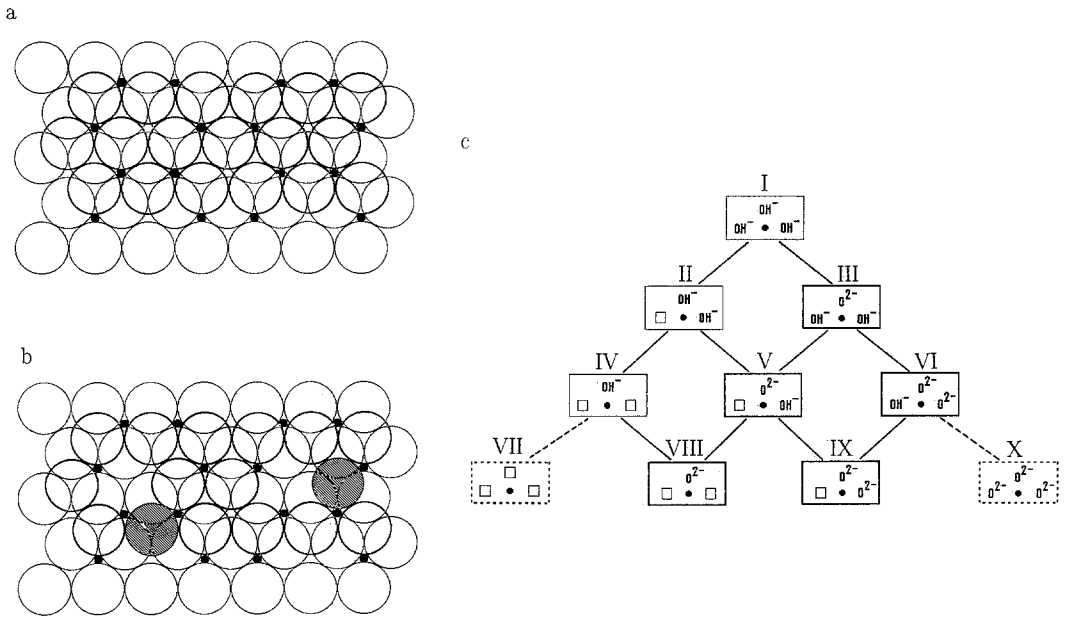

FIG. 1. Model for the generation of coordinatively unsaturated sites on a (001) surface of Cr_2O_3. (a) In hydrous atmosphere, the chromia surface is saturated with hydroxyl groups (large bold circles). (b) A coordinatively unsaturated site with an adjacent O^{2-} ion (shaded circles) is formed after a water molecule desorbs from the surface. (c) Several types of chromium surface sites are created by sequential steps of water desorption (top to bottom).

ions will be fivefold coordinated. When atmospheric water is admitted to this hypothetical cleavage plane, each Cr^{3+} ion will achieve coordinative saturation by adsorbing one H_2O molecule, followed by proton transfer from the water molecule to an adjacent oxide ion. As a consequence, the outer surface consists of a closely packed layer of hydroxide ions, as shown in Fig. 1a. Every Cr^{3+} ion in the top layer is coordinated by three oxide ions from the bulk and three hydroxide ions on the surface.

During activation at increasing temperatures a loss of physisorbed water is expected first, which will be complete at about 473 K. Subsequently, further water molecules are desorbed by condensation of surface OH^- groups:

$$2OH^- \rightarrow O^{2-} + H_2O.$$

This process generates coordinatively unsaturated Cr^{3+} surface species, as shown in Fig. 1b. The unsaturated Cr^{3+} ions are characterized by a high Lewis acidity. In this process, coordinatively unsaturated surface O^{2-} ions are formed as well, which act as strong Lewis bases.

The condensation of two OH^- ions creates a defect, as shown in Fig. 1b. The resulting Cr^{3+} species are shown in Fig. 1c (second row), i.e., two onefold coordinatively unsaturated Cr ions surrounded by OH^- ions and one saturated Cr ion with one unsaturated O^{2-} ligand. Starting from species II and III formed in this manner, the same sequence of reactions is possible again. The desorption of water from two adjacent OH^- ions generates a vacancy and a coordinatively unsaturated O^{2-} ion (species IV, V, and VI in the third row of Fig. 1c). If the condensation process of surface hydroxyls is repeated for a third time, species VIII and IX are generated. The formation of threefold coordinatively unsaturated Cr^{3+} ions (by dehydration of species IV) is unlikely on a (001) surface for energetical reasons.

To summarize, the model predicts (*4*) that

thermal activation of crystalline chromia will result in a surface featuring both coordination and ligand heterogeneity. Surface chromia species will differ in their coordination numbers (6, 5, or 4), and in the combination of OH^- or O^{2-} ligands.

3. EXPERIMENTAL

The preparation of crystalline and amorphous chromia samples used in this study has been reported in detail in part I of this study (*3*), and in Ref. (*16*).

FTIR experiments have been performed in a diffuse reflectance cell (Spectra-Tech Model 30-033) equipped with a temperature-controlled environmental chamber (Spectra-Tech Model 30-100); NaCl windows have been used. The crystalline and amorphous Cr_2O_3 were crushed and diluted with equal amounts of KBr.

In a first series of experiments, the influence of a thermal treatment on the catalyst surface was investigated on a Digilab instrument (Model FTS 80, run at 4 cm^{-1} resolution). The environmental chamber was constantly purged with a small flow of argon, from which oxygen had been carefully removed by passing it through a column filled with a $Cr(II)/SiO_2$ catalyst. The sample was slowly heated to 473 K under argon. Spectra were recorded at the temperatures indicated, allowing for an equilibration time of 3 min after each temperature step.

Adsorption and desorption experiments of O_2 and NH_3 were performed on a Perkin–Elmer instrument (Model 1710, run at 4 cm^{-1} resolution). Data handling and temperature program were controlled by a computer (Nixdorf, AT 386). The gas dosing system was designed to introduce three gases independently into the reaction chamber. Gas flows were adjusted to the desired level using volume flow controllers (Rota). Nitrogen (Linde, 99.999%) as the carrier gas, as well as oxygen (Linde, 99.999%) and ammonia (Linde, 99.999%), were used without further purification.

Diffuse reflectance spectra are usually presented as reflectivity changes R/R_0 or are reduced to the Kubelka–Munk function (*17*) $f(R/R_0) = [1 - (R/R_0)]^2/[2(R/R_0)]$, which is proportional to the absorption of the powder sample. This representation tends to emphasize intense features. To analyze relative intensity changes in a qualitative manner, we have plotted "pseudo-absorbance" spectra, $-\log(R/R_0)$.

Raman spectra were excited with the 514.5-nm line of an Argon ion laser (Spectra Physics Model 2025). For recording the Raman spectrum of crystalline chromia the laser power was adjusted to 50 mW. Laser-induced crystallization of amorphous chromia was studied by varying the laser power from 3 to 100 mW. The scattered radiation was dispersed in a triple spectrograph (SPEX triplemate Model 1877A), and registered with a multichannel detector based on a photodiode array and a cooled image intensifier previously described (*18*). The slit width was adjusted to correspond to a spectral resolution of ~5 cm^{-1}.

4. RESULTS

4.1. Thermal Treatment of α-Cr_2O_3

At room temperature, a broad and intensive band centered at 3450 cm^{-1} and a peak at 3695 cm^{-1} are observed in the OH stretching region of the DRIFT spectrum for α-Cr_2O_3 (Fig. 2, top). Upon rise of the temperature by 100°C, the intensity of the broad structure is strongly decreased, two maxima become visible at 3425 and 3300 cm^{-1}, and the peak at high frequency has been shifted to 3625 cm^{-1}. These trends are continued when the temperature is raised to 498 K: the maximum of the broad band is now found at 3450 cm^{-1}. When the sample is cooled to room remperature after treatment at 498 K for 1 h, the spectrum (Fig. 2, bottom) exhibits peaks at 3470 (broad), 3570 (weak), and 3610 cm^{-1}, as well as a shoulder at 3650 cm^{-1}.

The Cr=O stretching region around 1000 cm^{-1} is shown in Fig. 3b. At room temperature only a weak and broad maximum centered around 975 cm^{-1} is observed (top). After raising the temperature to 498 K a broad hump with a maximum at 980 cm^{-1} and a broad structure around 900 cm^{-1} ap-

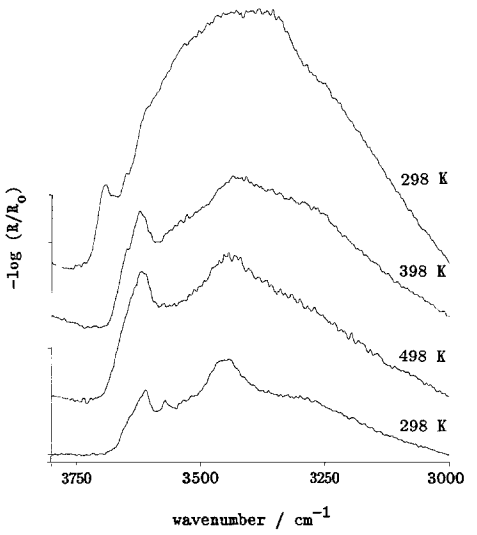

FIG. 2. Thermal treatment of an α-Cr_2O_3 surface. The OH stretching region of the DRIFT spectrum (R) is monitored as the temperature is raised. The bottom spectrum is observed after cooling to room temperature. KBr (Merck, spectroscopy grade) has been used to record the reference spectrum, R_0. Experimental details are indicated in the text.

pear in the spectrum. This spectrum evolves with time as shown in Fig. 3b. After 30 min, two separate absorption maxima at 995 and 960 cm^{-1} have developed; a further broad band at 880 cm^{-1} is discerned. After 60- and 90-min peaks at 1004 cm^{-1} (m), 992 cm^{-1} (m), 964 cm^{-1} (strong, with shoulders on both sides), and 931 cm^{-1} are seen in the spectrum. The lower-frequency band also features three peaks at 885, 875, and 865 cm^{-1}. Note that the relative intensities of the bands in the 1025–920 cm^{-1} region change upon holding the sample at 498 K. Zecchina *et al.* (*9*) have also observed this behavior and have attributed it to the mobility of chemisorbed oxygen at higher temperatures. Upon cooling the sample to room temperature (Fig. 3b, bottom), all peaks appear shifted to higher frequencies by 10 cm^{-1}, with the overall appearance of the spectrum unchanged. Positions of all the bands observed in this spectrum are summarized in Table 1; they are correlated with the results of Zecchina *et al.* (*9*) and of Carrot and Sheppard (*10*), who studied oxygen adsorption on reduced α-Cr_2O_3.

The overtone region corresponding to Cr=O stretches is shown in Fig. 3a. At room temperature no absorptions are detected. After heating to 498 K a weak band at 1955 cm^{-1} is formed. Upon holding the sample at this temperature, the band increases in intensity, and the maximum shifts to 1965 cm^{-1}. After cooling to room temperature a prominent band at 1975 cm^{-1}, a shoulder at 2015 cm^{-1}, and a weak broad structure at 1890 cm^{-1} are discerned.

4.2. *Oxygen Adsorption onto α-Cr_2O_3*

When oxygen is adsorbed on the surface of crystalline Cr_2O_3 at 473 K and a partial pressure of 100 mbar, changes in the Cr=O stretching region are observed, as shown in Fig. 4b. The bottom trace represents, as a reference point, the spectrum recorded at room temperature subsequent to the thermal treatment described in the previous section, but performed at a higher temperature, 623 K (compare with Fig. 3). Broad bands below 900 cm^{-1} have been assigned to combinations and overtones of lower frequency fundamentals modes (*19, 20*). The middle spectrum of Fig. 4b was observed at room temperature after 473 K oxygen treatment for 1 h. Changes are judged most easily from the difference spectrum plotted on a four times expanded scale (top trace). The absorption due to Cr=O stretching modes at 1015 and 998 cm^{-1} has been reduced (positive peaks in the difference spectrum), whereas absorption has increased at 980 and 960 cm^{-1}.

The changes discussed for the Cr=O fundamental vibrations are confirmed by monitoring the overtone region (Fig. 4a). The dominant overtone band at 1994 cm^{-1} (bottom) looses intensity after oxygen exposure (middle) and is slightly shifted to lower frequencies by 2 cm^{-1}. A weak feature visible at 2020 cm^{-1} in the thermally pretreated catalyst disappears upon O_2 adsorption, whereas a broad absorptive feature is formed around 1960 cm^{-1}. These changes

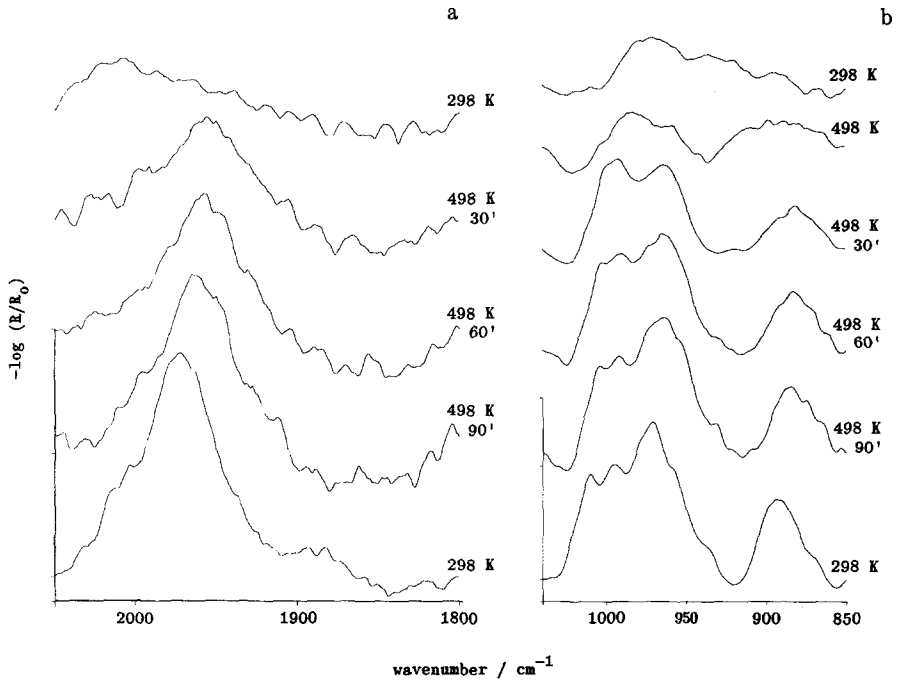

FIG. 3. Thermal treatment of an α-Cr_2O_3 surface. Changes in the Cr=O stretching region (b) and in the overtone region (a) are monitored as a function of time while the sample is held at 498 K. The final state after cooling to room temperature is shown in the bottom spectrum.

are judged most easily from the difference spectrum (top).

4.3. Thermal Treatment of Amorphous Cr_2O_3

At room temperature, the OH stretching region of the untreated amorphous chromia surface (Fig. 5) exhibits a broad band at 3475 cm^{-1} and a shoulder at 3685 cm^{-1}. When the temperature is raised to 398 and 498 K, the intensity of the broad structure is strongly decreased. A resolved band at 3645 cm^{-1} becomes visible, which shifts to 3635 cm^{-1} after cooling to room temperature.

Temperature-dependent changes in the Cr=O stretching region are presented in Fig. 6. Band intensities in the 1000 cm^{-1} range (Fig. 6b) are much weaker than those for α-Cr_2O_3 under all conditions. At room temperature, a weak absorption around 930 cm^{-1} is detected (Fig. 6b, top). After thermal treatment at 498 K for 1 h, a broad band with maxima around 975 and 996 cm^{-1} is observed (Fig. 6b, bottom). In the overtone region (Fig. 6a), a broad band extending from 1910 to 2040 cm^{-1}, with a maximum at 1960 cm^{-1}, is discerned after 1 h at 498 K.

4.4. Oxygen Adsorption onto Amorphous Cr_2O_3

Results of thermal treatment and oxygen adsorption onto amorphous chromia are shown in Fig. 7. The spectrum of amorphous chromia diluted with KBr, recorded at room temperature (Fig. 7) contains a very broad, structureless band centered around 560 cm^{-1} and a superimposed weaker absorption at 930 cm^{-1}. Two weak features at 1560 and 1430 cm^{-1} are assigned to surface bound carbonates; the presence of undissociated water is clearly recognized from the band at 1625 cm^{-1}. The diffuse reflectance spectrum of an undiluted amorphous chromia sample is shown in the second trace. The principal

TABLE 1

Cr=O Stretching Vibrations Observed on α-Cr_2O_3

Ref.(9)[a]	Ref. (4)[a]	Ref. (10)[a]	This work[b]
	1024 (sh)	1023 (m,sh)	1023 (m,sh)
1015 (s)	1016 (s)	1015 (s)	1013 (s)
		1003 (w,sh)	1004 (w)
995 (s)	995 (s)	995 (s)	995 (s)
	986 (m)	986 (m)	
980 (s)	980 (m)	980 (m,sh)	980 (s,sh)
		970 (m)	970 (s)
		960 (m)	960 (m)
		950 (w)	940 (w)
890 (m,b)	886 (m,b)		890 (m,b)

Note. (s) Strong; (m) medium; (w) weak; (sh) shoulder.
[a] Subsequent to O_2 adsorption.
[b] Subsequent to thermal treatment in argon.

reflectance minimum appears shifted (*21*, *22*) to 790 cm^{-1}. The absence of other strong bands (as observed for crystalline chromia) demonstrate the amorphous character of the sample.

Upon heating to 423 K in argon a very

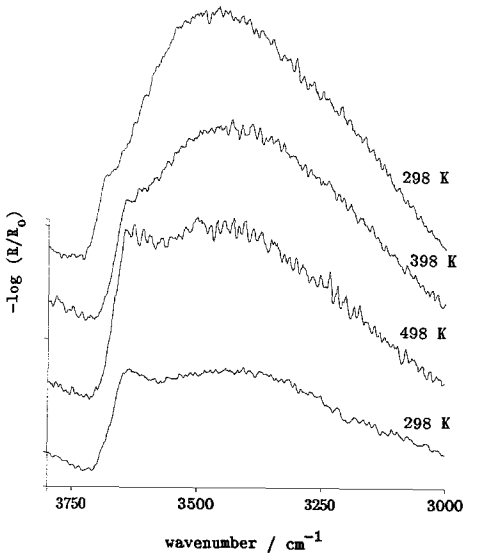

FIG. 5. Thermal treatment of an amorphous chromia surface. Changes in the OH stretching region of the DRIFT spectrum are monitored as the temperature is raised. The bottom spectrum is recorded after cooling to room temperature.

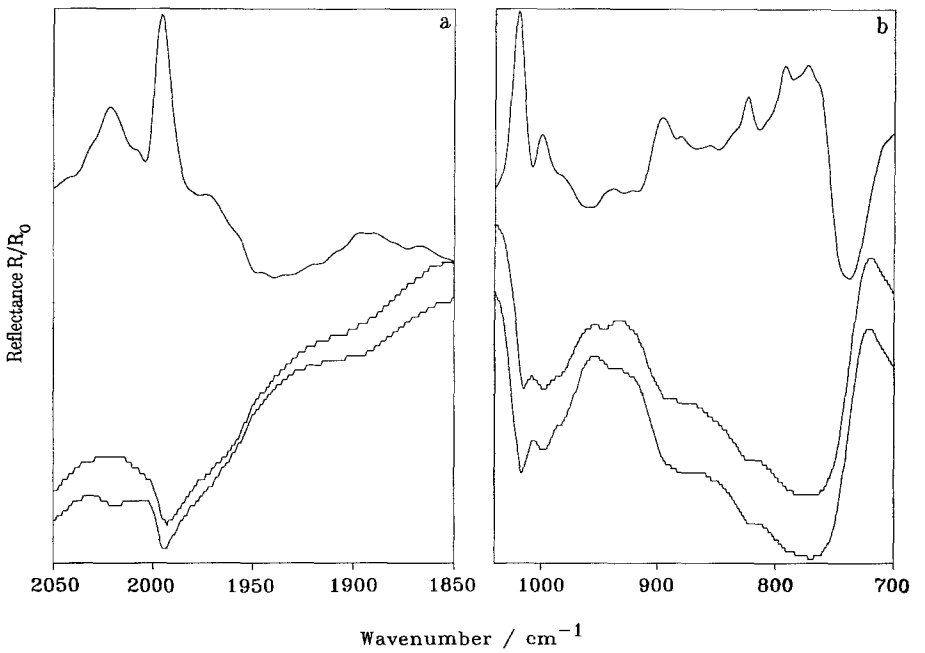

FIG. 4. Oxygen adsorption onto α-Cr_2O_3, as monitored in the Cr=O stretching (b) and overtone regions (a) of the DRIFT spectrum. All spectra have been recorded at room temperature. Bottom spectra represent the surfaces subsequent to thermal treatment at 623 K. The second spectrum from the bottom shows the state of the surface after oxygen adsorption at 473 K for 1 h. The difference of spectra (after and before oxygen adsorption) is shown in the top trace on a four times expanded scale.

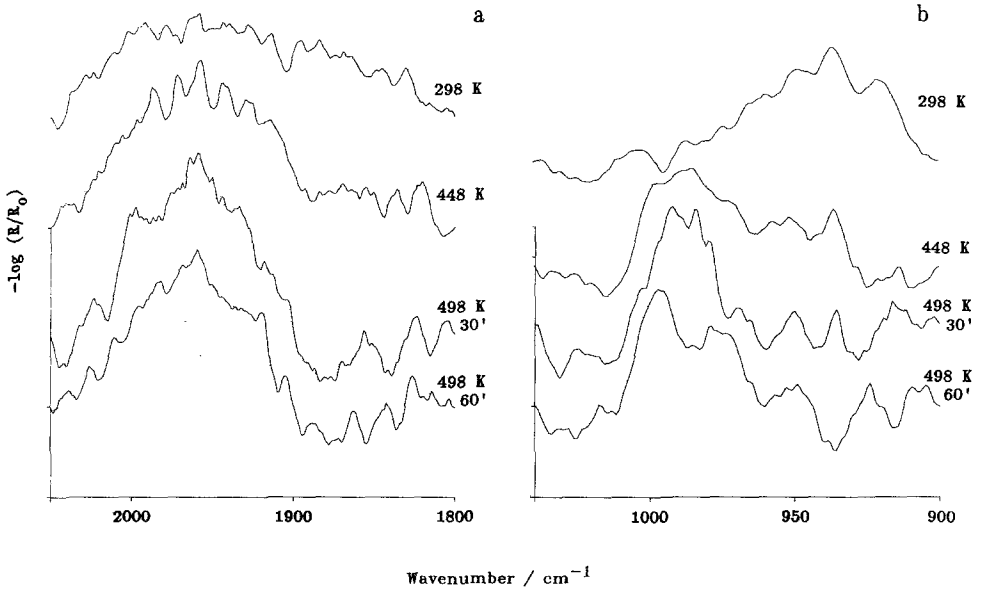

FIG. 6. Thermal treatment of an amorphous chromia surface. Changes in the Cr=O stretching region (b) and in the overtone region (a) are monitored as a function of time while the sample is held at 498 K.

intense absorption appears at 1625 cm^{-1}. It corresponds to the bending motion of adsorbed undissociated water molecules. The feature at 930 cm^{-1} looses intensity. Zecchina *et al.*(*9*) also observed a feature at 950 cm^{-1} that disappeared upon increase of the evacuation temperature, which they attributed to the bending mode of surface hydroxyl groups. The spectrum resulting after thermal treatment at 623 K in argon for 1 h is shown in the fourth trace from bottom. The bending mode of water at 1625 cm^{-1} and the band at 930 cm^{-1} have disappeared.

After exposure to oxygen at 473 K for 1 h, the spectrum (Fig. 7, top) develops a sharp band around 1000 cm^{-1} and weak shoulders around 670 cm^{-1} and 900 cm^{-1}. The structure of the band around 1000 cm^{-1} is of special interest because in previous investigations of amorphous chromia (*7*, *9*, *10*), only a broad and structureless absorption has been observed. The band is structured with reflectance minima at 1030, 1015, 1004, and 982 cm^{-1} and a shoulder toward lower frequencies (inset in Fig. 7).

4.5. Raman Investigations

The Raman spectrum of crystalline chromia is shown in the bottom trace of Fig. 8. Raman bands are observed at 616, 553, 349, and 293 cm^{-1}, in agreement with the literature (*23*). The spectrum of amorphous chromia recorded at a very low laser power ($\leq$5 mW) shows a broad structure extending from 500 to 900 cm^{-1}, with a maximum at 720 cm^{-1} and weak features at 550 and 1000 cm^{-1} (Fig. 8). A gradual increase of the laser power from 5 to 50 mW results in prominent changes: a sharp band at 550 cm^{-1} develops, the broad structure around 720 cm^{-1} decreases, and a broad shoulder at $\approx$820 cm^{-1} and two new bands at 338 and 303 cm^{-1} appear. The Raman spectrum of our crystalline sample (Fig. 8, top) resembles that of the commercial sample (bottom). From the spectra in Fig. 8 it appears that gradual crystallization of the amorphous sample is induced by laser heating of a small area (3 $\times$ 0.1 mm^2) at powers exceeding 10 mW (λ = 514.5 nm). As an indicator for this process, the band at 553 cm^{-1} may be used. Of partic-

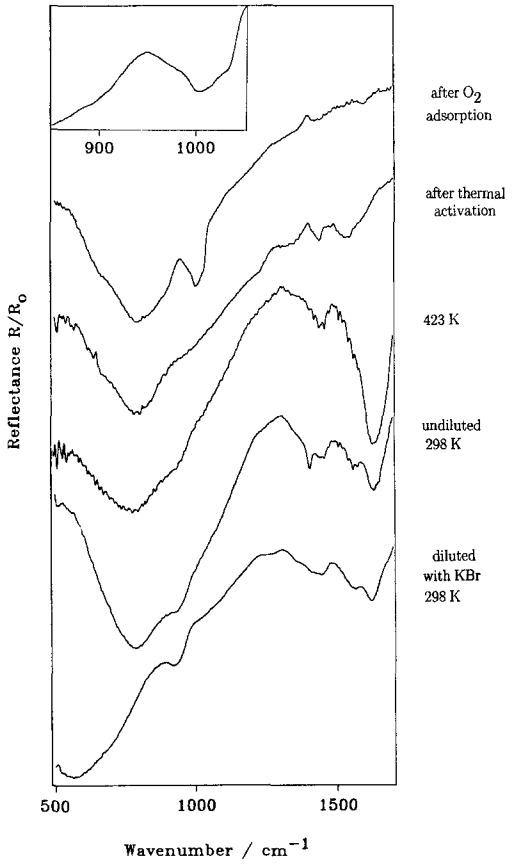

FIG. 7. Thermal activation (at 623 K) and oxygen adsorption on amorphous chromia. The fine structure of the Cr=O absorption band around 1000 cm^{-1} is shown as an insert.

ular interest in the Raman studies is the Cr=O stretching region from 900 to 1050 cm^{-1} shown in detail in Fig. 9, which is discussed below.

5. DISCUSSION

5.1. Crystalline Chromia

An inspection of the IR spectrum of crystalline chromia in the 3800–3000 cm^{-1} range after activation for 1 h at 473 K (bottom trace in Fig. 2) clearly demonstrates that the surface is still partially hydroxylated. Morishige *et al.* (*24*) have assigned IR absorption bands at 3590 and at 3420 cm^{-1} to the OH-stretching vibration of residual surface hydroxyls, after activation of α-Cr_2O_3 at 773 K in an inert atmosphere. According to Fig. 1 there are several species (I to VI) with an OH^- ligand in their coordination sphere, which can contribute to the distinct bands at 3610, 3570, and 3470 cm^{-1}. The large width of the latter band is caused by hydrogen bonding. Hadjiivanov *et al.* (*25*) have recently pointed out that replacement of an O^{2-} ligand by OH^-, i.e., attachment of an electron-withdrawing proton in the second coordination sphere, tends to increase the Lewis acidity of the central metal ion. Thus the presence of surface hydroxyl groups may be correlated with sites of strong Lewis acidity, to be discussed in part III of this study.

Spectra observed during thermal pretreatment of crystalline chromia (Fig. 3) show very good agreement with the work of Davydov *et al.* (*7*), Zecchina *et al.* (*9*), and Carrot and Sheppard (*10*), in particular in the Cr=O stretching region (Table 1). Note that in our experiment no oxygen adsorption was involved, but the surface was activated in a continuous stream of purified argon. In the spectrum recorded at room temperature subsequent to activation (bottom trace in Fig. 3), the most intensive bands are found at 970 and 890 cm^{-1}. The agreement with the literature suggests that the species created by reductive pretreatment followed by oxygen adsorption, as used in Refs. (*9*) and (*10*), and the surface structures resulting from the thermal treatment used in our work are quite similar. Both CO reduction and extensive thermal pretreatment will result in a dehydroxylated surface with coordinatively unsaturated sites. Zaki and Knözinger (*15*) state that the most abundant surface chromium species are singly unsaturated, but doubly and triply unsaturated sites are present as well. In terms of the model presented in Fig. 1, thermal treatment results in the exposure of species II, IV, V, VIII, and IX. The formation of twofold coordinatively unsaturated centers (species IV and VIII) appears less likely in view of the moderate temperatures used (473 K).

The observation of several bands in the

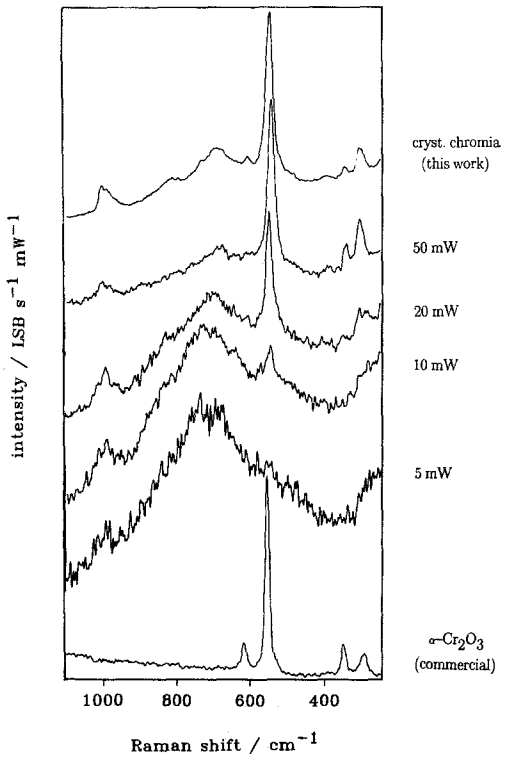

FIG. 8. Raman spectra from the surface of an amorphous chromia sample recorded at increasing laser powers. The bottom spectrum was obtained from commercial α-Cr_2O_3. The following traces represent spectra of amorphous chromia excited with the powers indicated. The top spectrum corresponds to crystalline chromia prepared as described in the experimental section.

1025–940 cm^{-1} interval after thermal pretreatment supports the conclusion (*8*) that several types of Cr=O bonds with bond order near 2 are present on the surface. As in our previous studies of supported V_2O_5 catalysts (*22*), the overtone region confirms this assignment. For thermally pretreated α-Cr_2O_3, the overtone region (Fig. 3a) also reveals several absorptions in agreement with the fundamental region (Fig. 3b). No overtones are observed at room temperature where the surface is fully hydroxylated.

Oxygen is dissociatively chemisorbed on a surface pretreated in this manner (*9, 10*). This process adds an additional oxygen ligand to the previously unsaturated sites. Thus, after oxygen adsorption we expect to observe species III and VI and perhaps the singly unsaturated species V and IX of Fig. 1. Species X, which was postulated by Zecchina *et al.*(*9*), would involve a formal oxidation state of chromium in excess of 6 and is therefore not considered in our mechanism.

Factors that are influencing the Cr=O bond order, and hence the oscillation frequency, are addressed next. A survey of spectroscopic data shows that a decrease in coordination number always leads to an increase in *M*=O vibrational frequency. As pointed out in Refs. (*5*) and (*9*), this "coordination heterogeneity" is the most important factor in an energetic differentiation of the various sites. "Ligand heterogeneity" (i.e., exchange of OH^- by O^{2-} or H_2O) causes a further minor differentiation.

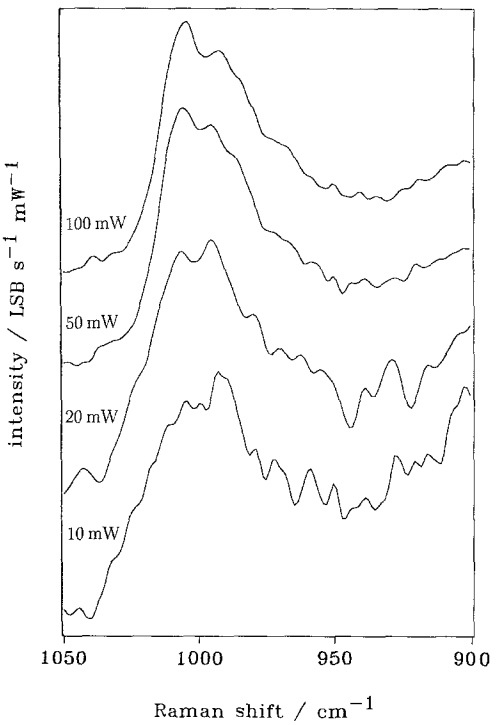

FIG. 9. Changes in the Cr=O stretching region observed during laser-induced crystallization of amorphous chromia. Spectra were recorded in the sequence from bottom to top as the laser power was increased from 10 to 100 mW.

From these results the following band classification is proposed. Twofold coordinatively unsaturated chromium ions (site VIII in Fig. 1) absorb at the highest frequency, i.e., 1023–1025 cm^{-1}. This feature is recognized only as a shoulder in Fig. 3b, as the formation of sites with two coordinative vacancies is infrequent during mild thermal treatment. Bands at 1015 and 998 cm^{-1} are attributed to chromium ions with one unoccupied coordination site (species V and IX in Fig. 1), which differ in one of their ligands (OH^- and O^{2-}, respectively). The most stable sites are those with no coordinative unsaturation, i.e., species III and VI in Fig. 1; the intensive signals at 986 cm^{-1} (shoulder) and 980 cm^{-1} (absorption maximum) observed in Fig. 3b are assigned to these species, which again are differentiated in frequency by ligand heterogeneity. The same bands have also been observed in Refs. (*7, 9, 10*).

We consider these assignments as tentative. They are supported by the observation that bands at 1015 and 995 cm^{-1} persist up to high temperatures and are greatly reduced in intensity by ethanol or water adsorption (*6, 7*). These bands must therefore correspond to chromium ions with at least one vacant coordination site. In contrast, bands around 980 cm^{-1} showed no sensitivity to the adsorption of Lewis bases and are therefore assigned to coordinatively saturated surface species.

The intensity increase around 890 cm^{-1} seen in Fig. 3b has also been observed by Zecchina *et al.* (*9*). These authors have argued that upon prolonged thermal pretreatment between 473 and 673 K, surface rearrangements are taking place due to the onset of surface mobility of the OH^- and O^{2-} ligands. It is conceivable that during this process, monomeric and polymeric structures are generated in which the chromium ions are tetrahedrally coordinated and are found in an oxidation state higher than +3. Such species would be characterized by bands at 890 and 970 cm^{-1} (*8*). (For an assignment of these vibrations, the spectrum of CrO_3 can be used as a reference (*27*). CrO_3 consists of chains of distorted tetrahedral CrO_4 coordination units. A strong band of CrO_3 observed at 980 cm^{-1} is attributed to the stretching vibration of the two free Cr=O groups, while a much broader band at 893 cm^{-1} is assigned to stretching modes of the Cr—O—Cr chains (*8*).) In our experiments the temperature was kept near the lower limit of the temperature interval where surface rearrangements are observed. In any case, the observation of two major absorptions at 980 and 890 cm^{-1} in our spectra clearly proves the existence of Cr=O double bonds, as well as the presence of oxygen ions in bridging positions between two chromium centers.

Changes occurring upon oxygen adsorption at 473 K onto the thermally pretreated surface can be assessed from the difference spectra presented in Fig. 4. Disappearing bands are discerned at 1015 and 998 cm^{-1}, as well as in the overtone region at 2022 and 1994 cm^{-1}. The evidence discussed above suggests that O_2 is dissociatively chemisorbed on the coordinatively unsaturated chromium sites, thereby producing saturated species. According to the scheme in Fig. 1, oxygen adsorption onto sites II and V would produce species of types III and VI. This process should therefore be associated with an increase in absorption intensity around 980 cm^{-1}, which is observed. Our results are in agreement with the findings of other authors (*6, 7, 9*) who reported the disappearance of Cr=O species absorbing at high frequencies and an absorption increase at lower frequencies, upon adsorption of Lewis bases like ethanol, water (*6, 7*), and N_2O (*9*). An intensity increase around 960 cm^{-1} could again be due to the development of tetrahedrally coordinated chromium centers due to enhanced oxygen surface mobility.

The intensity changes that we observe upon oxygen adsorption are weaker than those reported by other groups (*9, 10*). This is due to the fact that Zecchina *et al.* (*9*) performed their experiment on a surface that had been fully reduced, followed by

activation. In contrast, our catalysts had been pretreated by comparatively mild thermal activation in an atmosphere of oxygen-free argon prior to oxygen adsorption.

5.2. *Amorphous Chromia*

Results obtained in the 3800–3000 cm^{-1} range (Fig. 5) are in good agreement with the work of Zecchina *et al.* (*9*). At room temperature (top trace) a broad band centered at 3475 cm^{-1} due to undissociated water dominates the spectrum. This assignment is confirmed by the observation of a broad and intensive bending mode around 1620 cm^{-1} (Fig. 7, first and second trace from bottom). At 473 K this weakly bound water is progressively being desorbed, as evidenced also by thermal gravimetry and differential scanning calorimetry measurements (*12, 13*), and the stretching vibrations of surface hydroxyl groups at 3635 cm^{-1} become visible.

In the range of substrate skeletal motions (Fig. 7), only broad features at 800, 950, and $\approx$1100 cm^{-1} are observed at room temperature. Zecchina *et al.* (*9*) have attributed a broad feature observed between 900 and 1000 cm^{-1} to bending modes of surface hydroxyl groups. In agreement with Ref. (*9*), the 950 cm^{-1} band disappears upon raising the temperature.

To interpret the Raman spectrum of amorphous chromia (Fig. 8), reference data from some Cr(VI) compounds (*26, 27*) can be used. Spectral data on $Cr_2O_7^{2-}$, $Cr_3O_{10}^{2-}$, and $Cr_4O_{13}^{2-}$ ions in solid potassium compounds are reproduced in Table 2. An inspection of Table 2 reveals that all vibrations of Cr—O—Cr bridges may contribute to the broad band at 720 cm^{-1}. Laser heating of the sample causes further condensation of Cr—OH groups resulting in Cr—O—Cr bridges and the formation of small crystalline domains. Higher laser power (traces observed using 20 or 50 mW) promote fast crystallization of the amorphous sample. However, bands in the top spectrum are still broader than those in the crystalline reference compound (bottom trace).

TABLE 2

Raman Band Assignments for Chromium(VI) Oxyanions (Investigated as Solid Potassium Salts, from Refs. (*26*) and (*27*))

$K_2Cr_2O_7$	$K_2Cr_3O_{10}$	$K_2Cr_4O_{13}$	Assignment
	980	982	ν_{as} (CrO_2)
	945	957	ν_s (CrO_2)
945	903	936	ν_{as} (CrO_3)
902		887, 872, 818	ν_s (CrO_3)
770	818, 761	572	ν_{as} (CrOCr)
560, 234	562, 518	518, 490	ν_s (CrOCr)
382, 370	378	380, 332	δ (CrO_3)
220		209	δ (CrOCr)

Signals observed with the laser-crystallized sample in the Cr=O stretching region between 900 and 1050 cm^{-1} are of special interest. No signal in this region is observed with the commercial reference sample (Fig. 8). The sequence of changes induced by laser heating of amorphous chromia is shown in detail in Fig. 9. In the bottom trace recorded with 10 mW, one observes a structured band with a maximum at 980 cm^{-1} and a shoulder at 1005 cm^{-1}. When the laser power is increased to 20 mW, this shoulder develops into a pronounced peak. With further increase of the laser power to 50 and 100 mW the latter band becomes the most intensive feature of the spectral region. These observations indicate that incipient laser heating causes the desorption of physisorbed water and results in coordinatively saturated Cr=O surface species, characterized by a Raman band at 980 cm^{-1} (IR: 985 cm^{-1}). Increasing the laser power produces onefold coordinatively unsaturated sites that give rise to Raman bands at 1005 cm^{-1} and possibly at 990 cm^{-1}. In the IR spectra, the corresponding vibrations had been found at 1015 and 995 cm^{-1}. The generation of unsaturated chromia sites is paralleled by an increasing degree of crystallization of the amorphous chromia, as evident from Fig. 8.

These Raman spectroscopic results are useful to interpret the wide IR feature at 800 cm^{-1} in Fig. 7. This absorption parallels the broad Raman band observed around

720 cm^{-1} and is assigned to the stretching modes of Cr—O—Cr bridges (cf. Table 2). After thermal treatment at 623 K for 1 h, weak peaks are discerned in the IR spectrum at 1220, 1330, 1445, and 1550 cm^{-1}, as well as a shoulder at 1590 cm^{-1} (Fig. 7, fourth spectrum from bottom). In a study of CO_2 adsorption onto α-Cr_2O_3 (*9*), bands at the same frequencies have been assigned (*28*) to carbonate surface species bound to coordinatively unsaturated surface chromium ions. Ratnasamy *et al.* (*13*) have observed a band at 1550 cm^{-1} for a crystalline sample of $Cr(OH)_3(OH_2)_3$, which is characterized by short O—H—O bonds. The corresponding band in our spectrum may therefore be assigned to deformational motions of O—H—O bridges in the amorphous hydrous oxide.

Signals in the Cr=O stretching region observed after thermal activation of amorphous chromia are much weaker than those observed with α-Cr_2O_3. This is not a result of a lower density of chromium centers on the surface of amorphous chromia, which is more than compensated by its higher surface area. Rather it is due to the different bonding strength of labile oxygen. The results reported in part I (*3*) indicate that degassing in argon at 473 K for 1 h is sufficient to remove a part of the labile oxygen from the surface of crystalline chromia, whereas on the amorphous sample the labile oxygen density is only weakly influenced at this temperature.

It is interesting to correlate the Raman observations with the behavior of the two morphologies during thermal treatment. Thermal treatment of crystalline chromia at 473 K results in a variety of coordinatively unsaturated chromium sites. In addition to the removal of adsorbed water, labile oxygen species can easily be desorbed from the surface of α-Cr_2O_3. This process results in the well-resolved and strong IR bands shown in Fig. 3. In contrast, for amorphous chromia we observe only two weak and broad signals at 995 and 975 cm^{-1} after thermal treatment. The 995 cm^{-1} absorption is tentatively assigned to a onefold coordinatively unsaturated site, whereas the lower frequency peak corresponds to a saturated surface species. The different response of amorphous chromia to thermal treatment again suggests that oxygen species are more tightly bound in comparison with α-Cr_2O_3.

Changes occurring after oxygen adsorption at 473 K for 1 h are shown in Fig. 7 (top). The broad absorption at 800 cm^{-1} assigned above to stretching motions of Cr—O—Cr bridges remains unaltered during O_2 adsorption. This is in agreement with thermochemical measurements (*3, 4, 12, 13*) which gave evidence for a high activation energy in the formation of these links. The appearance of a clear feature around 1000 cm^{-1} with resolved fine structure shows that with amorphous chromia as well, surface Cr=O groups are formed. It is important to mention that the sample was still X-ray amorphous and the visual appearance remained black-green and unchanged. In agreement with Refs. (*6*) and (*9*), we conclude that dissociative oxygen adsorption is occurring on the surface of the amorphous chromia as well and that Cr=O groups are formed during this process. (Davydov *et al.* (*29*) have forwarded a different view from isotope labeling experiments; these authors assigned their 985 cm^{-1} feature to a dioxygen species, e.g., O_2^{2-}.) To our knowledge, this is the first observation of resolved Cr=O stretching vibrations in the spectra of amorphous chromia. The relative intensities of the individual features depend on oxygen partial pressure and adsorption temperature.

SUMMARY AND CONCLUSIONS

Coordinatively unsaturated sites and surface Cr=O groups are generated by thermal treatment of chromia surfaces, for crystalline as well as for amorphous Cr_2O_3. For α-Cr_2O_3, the degree of coordinative unsaturation depends on the temperature and on the duration of the thermal treatment, and can be monitored by observing the fine structure of the Cr=O fundamental stretching region. Twofold coordinatively unsatu-

rated chromium sites are characterized by frequencies of $\approx$1025 cm^{-1}. The assignment of bands around 1000 cm^{-1} to Cr=O stretching vibrations is established unambiguously from the observation of overtone absorptions in the 2000 cm^{-1} range.

Upon O_2 treatment at 473 K, the free surface coordination sites are occupied by the dissociative adsorption of oxygen. Coordinative unsaturation is reduced during this process, as reflected by changes in the Cr=O stretching region. After oxygen adsorption on crystalline chromia, the most intensive vibrations observed at 980 and 986 cm^{-1} are assigned to coordinatively saturated $Cr(O)(OH)_2$ and $Cr(O)_2(OH)$ surface species (III and VI in Fig. 1c).

In comparison to α-Cr_2O_3, amorphous chromia is characterized by an open and less compact structure. There are numerous residual Cr—OH groups, as well as characteristic bridges of the type O—H—O connecting two Cr^{3+} centers. Increasing the temperature results in condensation reactions of Cr—OH groups and the formation of weak Cr—O—Cr bridges. Desorption of water is observed in the course of this process. Thermal treatment at 473 K removes most of the labile oxygen on crystalline chromia, whereas these oxygen species are more tightly bound on the surface of amorphous chromia. Fine structure in the Cr=O stretching band upon oxygen adsorption provides information on the presence of different types of coordinatively saturated and unsaturated surface sites on amorphous Cr_2O_3.

Temperature-dependent changes in the surface structure of amorphous chromia have been studied by Raman spectroscopy. A very broad band centered around 720 cm^{-1} is observed. During the progressive laser-induced crystallization, coordinatively unsaturated surface Cr=O sites are created, as identified from the development of narrow, well-resolved features in the 1000 cm^{-1} region.

The importance of the chromia morphology with respect to the availability and strength of bonding of labile oxygen is apparent in view of the fact that SCR reactions on these catalysts are run in the temperature interval between 423 and 473 K. In this respect, the results from vibrational spectroscopy fully support the conclusions reached from the TPD experiments reported in part I: under the reaction conditions amorphous chromia has a labile oxygen site density higher than that of crystalline chromia and consequently is more active for the reduction of nitric oxide.

ACKNOWLEDGMENTS

M.S.-M. thanks the Verband der Chemischen Industrie for a graduate research fellowship. Financial support of this work by the Deutsche Forschungsgemeinschaft (SFB 213) and by the Schweizerische Nationalfonds is gratefully acknowledged.

REFERENCES

1. Flockenhaus, C., Wunderlich, E., Kainer, H., and Grimm, D., *Tech. Mitt.* **78,** 41 (1985); Bauerle, G. L., Wu, S. C., and Nobe, K., *Ind. Eng. Chem. Prod. Res. Dev.* **14,** 268 (1975); Bauerle, G. L., Wu, S. C., and Nobe, K., *Ind. Eng. Chem. Prod. Res. Dev.* **17,** 123 (1978); Wong, W. C., and Nobe, K., *Ind. Eng. Chem. Prod. Res. Dev.* **25,** 179 (1986); Niiyama, H., Murata, K., Ebitani, A., and Echigoya, E., *J. Catal.* **48,** 194 (1977).
2. Curry-Hyde, H. E., Musch, H., and Baiker, A., *Appl. Catal.* **65,** 211 (1990).
3. Curry-Hyde, H. E., Baiker, A., Schraml-Marth, M., and Wokaun, A., *J. Catal.* **133,** 397 (1992).
4. Burwell, R. L., Haller, G. L., Taylor, K. C., and Read, J. F., *in* "Advances in Catalysis" (D. D. Eley, H. Pines, and P. B. Weisz, Eds.), Vol. 20, p. 1. Academic Press, New York, 1969.
5. Knözinger, H., *in* "Advances in Catalysis" (D. D. Eley, H. Pines, and P. B. Weisz, Eds.), Vol. 25, p. 184. Academic Press, New York, 1976.
6. Shchekochikhin, Y. M., Panov, G.I., and Akulich, N. A., *Kinet. Katal.* **9,** 1086 (1968). [In English]
7. Davydov, A. A., Shchekochikhin, Y. M., Keier, N. P., and Zeif, A. P., *Kinet. Katal.* **10,** 919 (1969). [In English]
8. Barraclough, C. G., Lewis, J., and Nyholm, R. S., *J. Chem. Soc.,* 3552 (1959).
9. Zecchina, A., Coluccia, S., Cerruti, L., and Borello, E., *J. Phys. Chem.* **75,** 2783 (1971); Zecchina, A., Colùccia, S., Guglielminotti, E., and Ghiotti, G., *J. Phys. Chem.* **75,** 2774 (1971).
10. Carrot, P. J. M., and Sheppard, N., *J. Chem. Soc., Faraday Trans. 1* **79,** 2425 (1983).
11. Von Meyenburg, U., Siroky, O., and Schwarzenbach, G., *Helv. Chim. Acta* **56,** 1099 (1973).

12. Singh, K. K., Sarode, P. R., and Ganguly, P., *J. Chem. Soc., Dalton Trans.*, 1895 (1983).
13. Ratnasamy, P., and Leonard, A., *J. Phys. Chem.* **76,** 1838 (1972).
14. Scarno, D., Zecchina, A., and Reller, A., *Surf. Sci.* **198,** 11 (1988).
15. Zaki, M. I., and Knözinger, H., *J. Catal.* **119,** 311 (1989).
16. Curry-Hyde, H. E., and Baiker, A., *Ind. Eng. Chem. Res.* **29,** 1985 (1990).
17. Kortüm, G., "Reflexionsspektroskopie." Springer, Berlin, 1969.
18. Meier, M., Carron, K. T., Fluhr, W., and Wokaun, A., *Appl. Spectrosc.***42,** 1066 (1988).
19. Scarno, D., and Zecchina, A., *Spectrochim. Acta A* **43,** 1441 (1987).
20. Iglesias, I. E., Ocaña, M., and Serna, C. J., *Appl. Spectrosc.* **44,** 418 (1990).
21. Heilmann, A., Kampfrath, G., and Hopfe, V., *J. Phys. D: Appl. Phys.* **21,** 986 (1988); DOREMUS, R. H., *J. Appl. Phys.* **37**(7), 2775 (1966).
22. Schraml-Marth, M., Wokaun, A., and Baiker, A., *J. Catal.* **124,** 86 (1990).
23. Beattie, I. R., and Gilson, T. R., *J. Chem. Soc. A,* 980 (1970).
24. Morishige, K., Kittaka, S., and Katsuragi, S., *J. Chem. Soc., Faraday Trans. 1* **78,** 2947 (1982).
25. Hadjiivanov, K., Klissurski, D., and Davydov, A., *J. Chem. Soc., Faraday Trans. 1* **84,** 37 (1988).
26. Mattes, R., *Z. Naturforschung B* **24,** 772 (1969).
27. Mattes, R., *Z. Anorg. Allg. Chem.* **382,** 163 (1971).
28. Zecchina, A., Coluccia, S., Guglielminotti, E., and Ghiotti, G., *J. Phys. Chem.* **75,** 2790 (1971).
29. Davydov, A. A., Shchekochikhin, Y. M., and Keier, N. P., *Kinet. Katal.* **13,** 980 (1972). [In English]